Zhou, X., Lai, D., and Chen, Q. 2021. "Evaluation of thermal sensation models for predicting thermal comfort in dynamic outdoor and indoor environments," *Energy and Buildings*, 238: 110847.

Evaluation of thermal sensation models for predicting thermal comfort in dynamic outdoor and indoor environments

Xiaojie Zhou[a], Dayi Lai[b*], Qingyan Chen[c]
[a]*Tianjin Key Laboratory of Indoor Air Environmental Quality Control, School of Environmental Science and Engineering, Tianjin University, Tianjin 300072, China*
[b]*Department of Architecture, School of Design, Shanghai Jiao Tong University, Shanghai 200240, China*
[c]*School of Mechanical Engineering, Purdue University, West Lafayette, IN 47907, USA*

GRAPHICAL ABSTRACTS

This paper evaluated five thermal sensation models for predicting thermal comfort in dynamic outdoor and indoor environments.

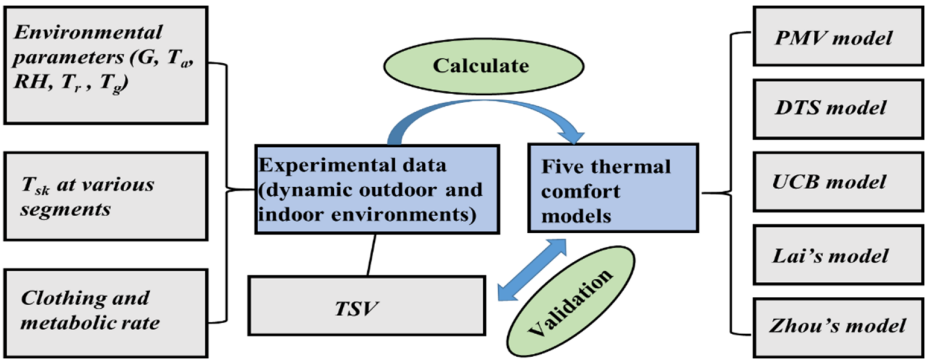

ABSTRACT

Thermal sensation models are commonly used to assess thermal perception in various indoor environments. Our previous work developed a new model to predict thermal sensation in cars that uses gradual change in thermal load on the face, sudden change in solar radiation on the face, mean skin temperature and outdoor air temperature as predictors. The present investigation selected 11 outdoor scenarios and 20 indoor scenarios from the literature to further verify the accuracy of the thermal sensation model. Four other thermal models, the predicted mean vote (PMV) model, the dynamic thermal sensation (DTS) model, a model from the University of California, Berkeley (UCB), and a transient outdoor thermal comfort model (Lai's) were compared with the new model for the 32 scenarios. The results confirmed the validity of the new model in an outdoor environment with sudden change in solar radiation. The new model was able to predict the trend of thermal changes, but the accuracy was not as good as that of the PMV model in an environment with indoor temperature gradient/sudden changes.

Keywords: Model validation, Non-uniform, Transient

1. Introduction

People are often exposed to transient thermal environments in their daily lives[1]. When moving between spaces—for example, from one room to another, from indoors to outdoors, from sun to shade—people experience sudden changes in air temperature, solar radiation, and wind speed. They also experience transient thermal conditions when occupying spaces with widely varying temperatures, e.g., in a moving car after the air conditioner is turned on[2] or in a kitchen space during cooking activities[3]. With the prevalence of transient thermal

environments, much effort has been devoted to developing dynamic thermal comfort models for different scenarios. For example, the dynamic thermal sensation (DTS) model was developed by Fiala[4], [5] for transient and spatially uniform indoor thermal environments. A model developed by the University of California, Berkeley (UCB) was aimed at predicting thermal sensation in a non-uniform indoor environment[6], [7]. Lai et al.[8], [9] developed a model (hereafter "Lai's") for outdoor dynamic thermal environments. Our previous work[10] also developed a model (hereafter "Zhou's") to predict thermal sensation in a transient and non-uniform vehicular thermal environment.

All the above models could be used for dynamic thermal conditions, although they were developed on the basis of data from specific scenarios. The main purpose of this study was to test these thermal sensation models, including the one that we previously developed, for a number of additional scenarios from the literature in order to identify the best model.

2. Research Method

This section introduces the above-mentioned models, including our model for vehicular environments[10]. Next, outdoor and indoor cases with transient thermal environments from the existing literature are used to evaluate the models. Finally, the section presents the criteria for assessing these thermal comfort models.

2.1 Evaluated thermal sensation models

This study evaluated five models, namely, the model for vehicular environments by Zhou, the predicted mean vote (PMV) model, the DTS model, the UCB model, and Lai's model.

Zhou's model[10] predicts thermal sensation vote (TSV) in cars by using the gradually changing thermal load of a face segment, $TL_g\ (face)$, the suddenly changing thermal load of the face caused by solar radiation, $TL_s\ (face)$, the mean skin temperature, $T_{sk,m}$, and the outdoor air temperature, T_{out}, as predictors. Equation (1) is the mathematical expression of Zhou's model.

$$TSV = 0.01 \cdot TL_g(face) + 0.216 \cdot T_{sk,m} - 7.352 + \frac{\Delta TL_s(face)}{-3.0714 \cdot T_{out} + 166.8} \quad (1)$$

The model can be separated into two parts. The first three terms on the right side of the equation represent the influence of gradually changing parameters (*TSV1*), and the last term represents the influence of sudden changes in solar radiation (*TSV2*).

The predicted mean vote (PMV) model[11] was based on the human energy budget under steady-state thermal conditions. The PMV model was regressed against metabolic rate (*M*) and thermal load (*TL*) calculated by six environmental and human parameters (air temperature, humidity, air velocity, mean radiant temperature, clothing insulation, and metabolism rate).

The dynamic thermal sensation (DTS) model was developed by Fiala[4], [5] by regressing a large amount of pre-existing human subject test data. The DTS model depends on the error signal from the skin ($\Delta T_{sk,m}$), error signal from the head core (ΔT_{cr}), and the rate of change of the mean skin temperature ($dT_{sk,m}/dt$). $dT_{sk,m}(-)/dt$ is negative rates of change of the mean skin temperature as a dynamic signal influencing regulatory responses against cold, i.e. shivering and vasoconstriction; $(dT_{sk,m}(+)/dt)_{max}$ is positive changing rate of mean skin temperature as a dynamic signal influencing regulatory responses against hot, i.e. sweating and vasodilation.

The University of California, Berkeley (UCB) model[6], [7] was originally intended for studying thermal comfort in a non-uniform environment. The UCB model was developed by building up a regression model between collected thermal sensation vote, thermal comfort

vote, local skin temperature, core temperature and the rate of change of skin and core temperatures.

Lai's model[8], [9] was based on the regression of a large amount of experimental data obtained under different outdoor thermal environments. The Lai's model uses the thermal load (*TL*) to evaluate the thermal environment, and the mean skin temperature, and its change rate to consider dynamic changes in the thermal state of the human body.

Table 1 summarizes the air temperature ranges under which the data was obtained for these models and the model input parameters[12].

Table 1. General information about the thermal sensation models.

Model	Air temperature range (ºC)	Input parameters*	References
PMV	19.0-28.0	*TL, M*	Fanger [11], Chap. 4, Eqs. (25), (40) and (41)
DTS	10.0-48.0	$\Delta T_{sk,m}$, ΔT_{cr}, $dT_{sk,m}/dt$	Fiala et al. [5], Eqs. (1)–(10)
UCB	20.0-32.0	$\Delta T_{sk,m}$, $\Delta T_{sk,i}$, $dT_{sk,i}/dt$, dT_{cr}/dt	Zhang et al. [6], Eq. (5)
			Zhang et al. [7], Section 1.3.1
Lai's	0.0-35.0	$\Delta T_{sk,m}$, *TL*, $dT_{sk,m}/dt$	Lai et al. [9], Eqs. (3) and (4)
Zhou's	0.0-50.0	$T_{sk,m}$, TL_g*(face)*, TL_s *(face)*	Zhou et al. [10]

*TL = thermal load, M = metabolic rate, $T_{sk,m}$ = mean skin temperature, T_{cr} = core temperature, $T_{sk,i}$ = skin temperature for the ith segment, dT_{cr}/dt, $dT_{sk,i}/dt$ and $dT_{sk,m}/dt$ = rates of change of core temperature, skin temperature and mean skin temperature, respectively, for the ith segment, TL_g *(face)* = thermal load of face caused by heat transfer other than solar radiation, TL_s *(face)* = thermal load of face caused by solar radiation. Parameters marked by a delta (Δ) are error signals, i.e., the difference between the parameter under the actual conditions and that under thermo-neutral conditions.

2.2 Cases for validation

In order to evaluate the performance of the models when applied to different dynamic thermal environments, this investigation identified a number of cases with human subject tests from peer-reviewed journals. The cases cover a wide range of environmental conditions, activity levels and clothing insulation levels. To ensure reliable environmental and personal input parameters, most of the validation cases we choose were with a minimum of six subjects and with detailed experimental protocols. We also contacted some of the authors directly to obtain additional information.

The cases were divided into outdoor and indoor ones. Table 2 shows 11 exposure scenarios typically encountered in outdoor spaces, such as shuttling between sun and shade (outdoor cases 1-5), exercising under gradually changing solar radiation (outdoor case 6), and standing under different solar radiation intensities (outdoor case 7).

Table 2. Description of the outdoor cases, with the ranges of environmental and personal parameters.

No.	Ref.	Type	Environmental parameters*					Subjects' personal parameters	
			T_a (ºC)	G (W/m^2)	V_a (m/s)	SVF	RH (%)	Number of subjects	Activity (met)
1	[13]	Sun–Building/ pergola shade	32.0-33.0	32-846.6	0.8-1.5	0.02-0.65	50.0	7	1.1
2	[14]	Sun–Building shade	0.0-35.0	130-1000	0.0-4.0	0.65-0.69	25.0-90.0	64	1.3
3	[15]	Sun–Umbrella shade	34.0	185-970	1.2	0.02-0.65	45.0	11	1.3
4	[16]	Sun–Umbrella shade	22.0-30.0	0-1000	0.0-2.0	0.02-0.65	-	10	1.3
5	[17]	Sun–Tree shade	30.0-36.0	600-850	1.0-1.7	0.02-0.66	25.0-48.0	6	1.3
6	[18]	Low solar radiation–exercising	30.8	0-306	2.1	0.65	57.0	10	4.0[19]
		Medium solar radiation–exercising	30.4	0-592	1.8	0.65	51.0	10	4.0[19]
		High solar radiation–exercising	31.0	0-1072	2.1	0.65	50.0	10	4.0[19]
7	[14]	Sun–Cloud cover–standing	34.8	2-400	0.3	0.02-0.65	28.5	1	1.3
		Sun–Cloud cover–standing	34.7	3-1000	1.3	0.02-0.66	30.5	1	1.3
		Sun–Cloud cover–standing	34.2	170-400	0.3	0.65	56.0	2	1.3

*T_a = air temperature, G = total radiation, V_a = air velocity, SVF = sky view factor, RH = relative humidity.

Although many indoor studies reporting thermal sensation votes can be found in the literature[20], [21], simultaneous measurements of thermo-physiological parameters are rare because of ethical concerns and the higher costs of such measurements. To make the validation more accurate, we selected indoor cases that reported not only thermal sensation votes but also detailed measurements of environmental parameters and skin/core temperature. Table 3 shows a total of 20 indoor exposure scenarios with dynamic thermal conditions. Case 1 and 2 were transient with air temperature ramps, while cases 3–8 were transient with step changes.

Table 3. Description of the indoor exposure scenarios, with the ranges of environmental and personal conditions.

No.	Ref.	Type	Environmental parameters*				Subjects' personal parameters		
			T_a (ºC)	T_r (ºC)	V_a (m/s)	RH (%)	Number of subjects	Activity (met)	I_{cl} (clo)
1	[22]	T_a-ramp change	33/25	T_a	0.1	50.0	7	1.1	0.30
2	[23]	T_a-ramp change	24/32	T_a	0.1	50.0	16	1.1	0.58

		T_a-ramp change	24/16	T_a	0.1	50.0	16	1.1	0.58
3	[24] [25]	T_a-step change	22-37-22	T_a	<0.1	40.0-70.0	24	1.1	0.50
		T_a-step change	26-37-26	T_a	<0.1	40.0-70.0	24	1.1	0.50
		T_a-step change	32-37-32	T_a	<0.1	40.0-70.0	24	1.1	0.50
4	[26]	T_a-step change	26-32-26	T_a	0.1	50.0	30	1.1	0.57
		T_a-step change	26-29-26	T_a	0.1	50.0	30	1.1	0.57
		T_a-step change	26-23-26	T_a	0.1	50.0	30	1.1	0.57
		T_a-step change	26-20-26	T_a	0.1	50.0	30	1.1	0.57
5	[27]	T_a-step change	32-25-32	T_a	0.1	60.0	20	1.1	0.50
		T_a-step change	30-25-30	T_a	0.1	60.0	20	1.1	0.50
		T_a-step change	28-25-28	T_a	0.1	60.0	20	1.1	0.50
6	[28]	T_a-step change	29-18-29	T_a	<0.1	<40.0	3	1.1	0.04
		T_a-step change	28-48-28	T_a	<0.1	<40.0	3	1.1	0.04
7	[29]	T_a-step change	32-24	T_a	<0.2	60.0	16	1.1	0.50
		T_a-step change	28-24	T_a	<0.2	60.0	16	1.1	0.50
		T_a-step change	20-24	T_a	<0.2	60.0	16	1.1	0.50
8	[30]	T_a-step change	30-20	T_a	<0.1	50.0	10	1.1	0.20
		T_a-step change	10-20	T_a	<0.2	50.0	11	1.1	1.12

*T_a = air temperature, T_r = mean radiant temperature, V_a = air velocity, RH = relative humidity, I_{cl} = clothing thermal resistance.

2.3 Index for model evaluation

The performance of the five models was assessed on the basis of the root-mean-square error (*RMSE*), which is an indicator of a model's precision. The goodness-of-fit of the simulation results to the experimental data can be assessed practically by comparing *RMSE*. The *RMSE* was calculated according to the following equation:

$$RMSE = \sqrt{\frac{\sum\left(x_{actual} - x_{prediction}\right)^2}{n}} \quad (2)$$

where x_{actual} is the thermal sensation data collected from selected experiments as listed in Tables 2 and 3, $x_{prediction}$ is the predicted thermal sensation, and n is the number of observations.

3. Results

This section presents the performance evaluation of Zhou's model for the indoor and outdoor cases. The performance of the other four models (PMV, DTS, UCB, and Lai's) is also shown for comparison.

3.1 Validation of outdoor cases

Due to the limited length of this article, we present detailed results for four typical cases. The complete evaluation results are then summarized. In outdoor case 1, subjects were shuttled between sun and shade with sitting posture. Outdoor case 4 had subjects shuttled between sun and shade with standing posture. In outdoor case 6, human subjects performed

exercises under different solar radiation intensities. Outdoor case 7 was similar to case 6, but the subjects maintained a standing posture.

Outdoor case 1: Sun–building/pergola shade with sitting posture

This investigation first used a case designed for evaluating thermal comfort during summer in a humid subtropical region[13]. The experiment was conducted on the campus of Daido University in Nagoya, Japan. Three outdoor experimental scenarios were set up for the study. Sensors were installed 15 min before the measurement began, at which point the subjects had become accustomed to the initial state. In setting 1, subjects sat in the shade of a building. In setting 2, subjects sat under direct sun. In setting 3, subjects sat in the shade under a pergola. Each subject was moved from experimental setting 1 to setting 2, and then to setting 3. In each setting, subjects sited for 20 min and evaluated the thermal environment every five minutes using a questionnaire. Table 4 shows the changes in air and globe temperatures with time, as well as global solar radiation, air velocity and relative humidity measured in the building shade, sunlight, and pergola shade.

Table 4. Description of outdoor case 1

Setting	T_a (ºC)	T_g (ºC)	G (W/m^2)	V_a (m/s)	SVF	RH (%)	I_{cl} (clo)	$T_{sk,m}$ (ºC)
Building shade	31.9	31.7	32	1.5	0.02	53.0	0.31	-
Sun	32.9	48.4	847	0.8	0.65	50.3	0.31	-
Pergola shade	32.9	34.5	58	1.2	0.05	50.0	0.31	-

*T_g = global temperature, I_{cl} = clothing thermal resistance.

Figure 1 compares the actual thermal sensation with the sensation predicted by Zhou's, PMV, DTS, UCB and Lai's models. Table 5 provides the actual thermal sensation and the thermal sensation predicted by the five models in different experimental settings.

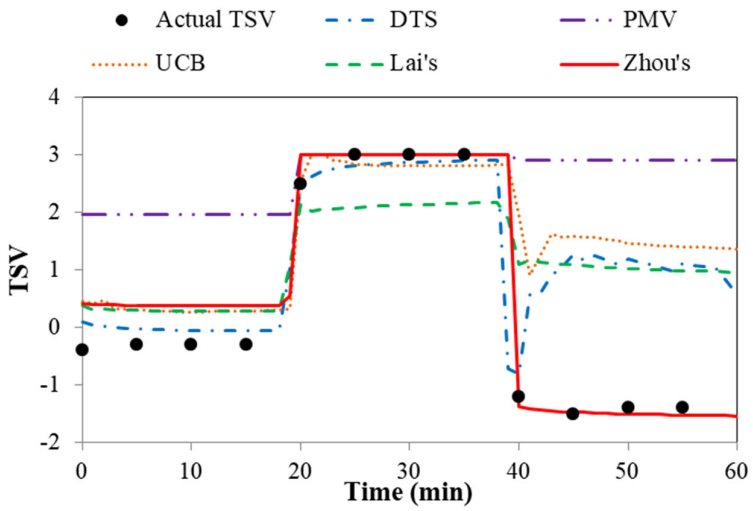

Fig. 1. Comparison of the actual thermal sensation votes with the predicted votes for outdoor case 1 as specified in Table 2.

Table 5. Actual thermal sensation and the thermal sensation predicted by the five models in different experimental settings.

Setting	Actual *TSV*	Lai's	PMV	UCB	DTS	Zhou's
Building shade (t = 0-20 min)	-0.3	0.3	1.9	0.3	0.0	0.4
Sun (t = 20-40 min)	3.0	2.1	3.0	2.8	2.9	3.0
Pergola shade (t = 40-60 min)	-1.5	1.0	2.9	1.5	1.0	-1.5

In order to analyze the accuracy of the predictions by the various thermal sensation models, we must first determine the input parameters of these models. Figure 2(a) shows the average skin temperature, $T_{sk,m}$, and the rate of change of average skin temperature, $d(T_{sk,m})/dt$. Figure 2(b) shows the the gradual and sudden thermal loads of the face, TL_g *(face)* and TL_s *(face),* respectively, and of the whole body, TL_g *(all)* and TL_s *(all)*.

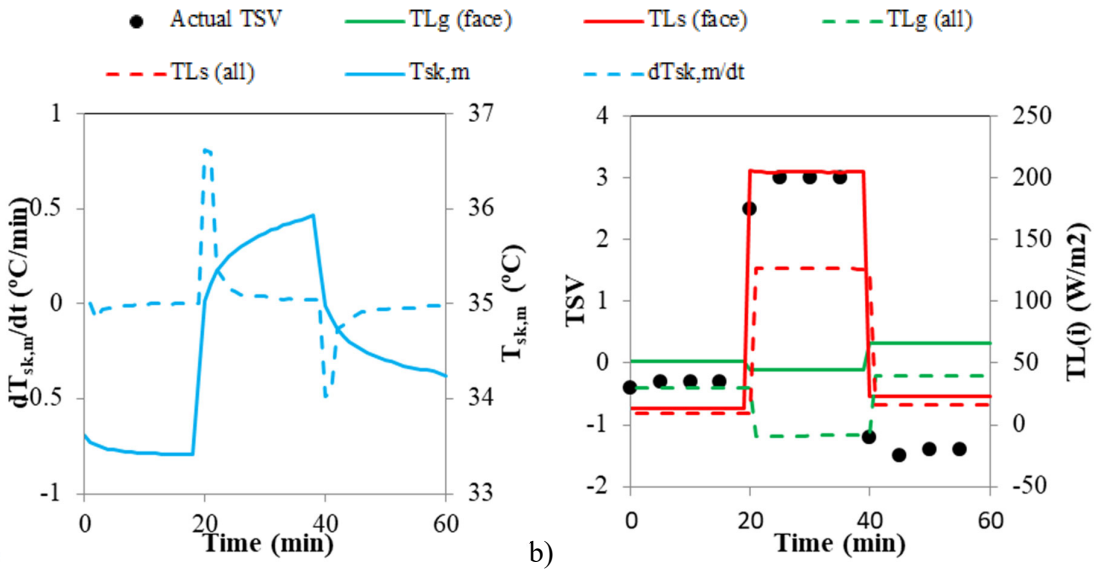

Fig. 2. Input parameters for different thermal comfort models for outdoor case 1 as specified in Table 2.

The PMV model predicted an overly high *TSV*. This was mainly due to the large outdoor thermal load *TL (all)* value, which was a sum number of TL_g *(all)* and TL_s *(all)*. As shown in Figure 2(b), the values of *TL (all)* were 38.2, 114.0, and 53.1 W/m^2, respectively, for the three outdoor environments. *TL (all)* changes between -54.0 and 54.0 W/m^2, and the PMV changes between -3.0 and +3.0, for a metabolic rate of 1.1 met. Thus, the thermal sensation values predicted by the PMV model were 1.9, 3.0 and 2.9, respectively, for the three outdoor settings. The predicted values were much larger than the actual ones in settings 1 and 3. For setting 2, the predicted and actual *TSV* reached the upper limit of +3. This finding was in accordance with previous results from Nikolopoulou et al.[31], Thorsson et al.[32], and Lai et al.[33]. In those field studies, the PMV model over-predicted the outdoor thermal sensation considerably.

The other four models correctly reproduced the trend of change, but the values differed considerably. The prediction errors of the DTS and UCB models were less than 0.6 units for outdoor settings 1 and 2. For the pergola shade (setting 3), however, the predicted *TSV* values were 2.5–3.0 units larger than the actual *TSV*. Because the two models used skin and core temperatures as input, and these parameters changed little while the solar radiation had a down-step change, the change in *TSV* caused by sudden changes in solar radiation was not reflected in the calculated *TSV*.

For Lai's model, *TL (all)* changed from 38.2 to114.0 W/m^2, causing a one-unit increase in thermal sensation with the up-step change in solar radiation. *TL (all)* changed from 114.0 to 53.1 W/m^2, causing a 0.7-unit drop in thermal sensation with the solar radiation down-step change. Thus, the poor prediction accuracy of Lai's model may have been due to underestimation of the effect of changes in solar radiation.

Zhou's model provided the best prediction. Figure 3 shows the *TSV1* and *TSV2* calculated by Zhou's model. The *TSV1*, which reflects the influence of TL_g *(face)* and $T_{sk,m}$, made contributions of 0.4, 0.8, and 0.8 units, respectively, in the three outdoor settings. The *TSV2*, which reflects the influence of sudden changes in solar radiation, made contributions of0.0, 2.4, and -2.3 units, respectively, for the three settings. The reason for the high accuracy of Zhou's model is that it successfully reflects the influence of sudden changes in solar radiation on thermal sensation.

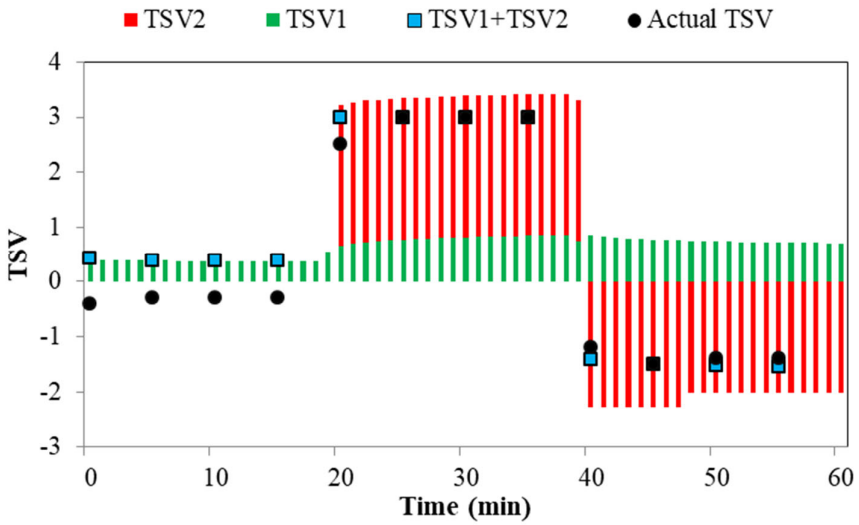

Fig. 3. Comparison of actual thermal sensation values with those contributed by different parts of Zhou's model for outdoor case 1 as specified Table 2.

Please note that the actual TSV was -0.3, indicating a neutral-to-slightly-cool state for outdoor setting 1, whereas the *TSV* values predicted by the five models were all greater than 0, indicating a neutral-to-slightly-warm state. This difference may have occurred because outdoor subjects were sensitive to wind speed, and a higher wind speed (1.5 m/s) would have decreased their thermal sensation.

Table 6 presents the *RMSE* for the five models. The performance of the PMV model was the worst, and that of Zhou's model was the best. The *RMSE* values for all models except Zhou's were greater than one, which indicates that those models are not well-suited for such a scenario.

Table 6. *RMSE* of the five thermal comfort models for outdoor case 1.

	Lai's	PMV	UCB	DTS	Zhou's
Outdoor case 1	1.52	2.81	1.77	1.34	0.44

Outdoor case 4: Sun–umbrella shade with standing posture

Outdoor case 4 was conducted in an urban park in Tel Aviv, Israel. The effect of solar radiation on thermal sensation was examined for two settings, with a step-like pattern of change from sunshine to shade. Ten subjects stood still and remained quiet in the sun for 15 minutes and then stood under umbrella shade for 15 minutes. In each 'setting' the subjects were asked to get used to the condition for 10 min, and to fill in the questionnaire in the remaining 5 min. The procedure was repeated from 07:30 to 18:30 local solar time, and the tests were conducted on May 17 and June 1, 2000. Thus, a total of 46 sets of *TSV* in the sun and under the shade were obtained.

For this outdoor thermal comfort experiment, the authors did not record the skin temperature of subjects. When using this example for analysis, the present study assumed that the skin temperature of each subject was 34.0 ºC, and that it did not change as the subject was shuttled from the sun to the shade. Therefore, for this case, the DTS and UCB models, with the skin temperature and the rate of change of skin temperature as input parameters, could not be used for comparison.

With the assumption that the subjects' skin temperature did not change, we used the ΔTSV *(Actual)*, which is the change in thermal sensation when shuttling from sun to shade, for model validation. The ΔTSV can be calculated by:

$$\Delta TSV = TSV(sun) - TSV(shade) \tag{3}$$

For Zhou's model, then, using Equation (1),

$$\Delta TSV(Zhou's) = 0.01 \cdot \Delta TL_g(face) + 0.216 \cdot \Delta T_{sk,m} + \frac{\Delta TL_s(face)}{-3.0714 \cdot T_{out} + 166.8} \tag{4}$$

Since $\Delta TL_g(face) = 0$ and $\Delta T_{sk,m} = 0$, Equation (4) becomes:

$$\Delta TSV(Zhou's) = \frac{\Delta TL_s(face)}{-3.0714 \cdot T_{out} + 166.8} \tag{5}$$

The difference in *TSV* between sun and shade calculated by the PMV model can be expressed as:

$$\Delta TSV(PMV) = [0.303 \cdot \exp(-0.0368M) + 0.028] \cdot \Delta TL(all) \tag{6}$$

Since $\Delta TL_g(all) = 0$, Equation (6) becomes:

$$\Delta TSV(PMV) = [0.303 \cdot \exp(-0.0368M) + 0.028] \cdot \Delta TL_s(all) \tag{7}$$

Meanwhile, the sun-shade *TSV* difference calculated by Lai's model is:

$$\Delta TSV(Lai's) = 3\left(\frac{2}{1+\exp(B_1 \cdot TL(shade)} - \frac{2}{1+\exp(B_1 \cdot TL(sun)}\right) \tag{8}$$

Figure 4 depicts the difference in the actual thermal sensation, ΔTSV *(Actual)*, the difference in the sudden thermal loads on the face caused by solar radiation, ΔTL_s *(face)*, and the difference in the sudden thermal loads on the whole body caused by solar radiation, ΔTL_s *(all)*, between the two outdoor settings. Figure 4(a) displays the results of the experiment on May 17, while Figure 4(b) shows the results of the experiment on June 1. A total of 23 sets of experimental data were obtained every day. The ΔTL_s *(face)* varied from 0 to 134.2 W/m^2 and ΔTL_s *(all)* from 0 to 95.5 W/m^2. At 18:30, in the early evening, the difference in thermal sensation between the open area and shade, ΔTSV *(Actual)*, was close to 0. This explains the fact that the sudden thermal loads on the face TL_g *(face)* and whole-body TL_s *(all)* were almost the same in open and shaded areas when the sun had gone down.

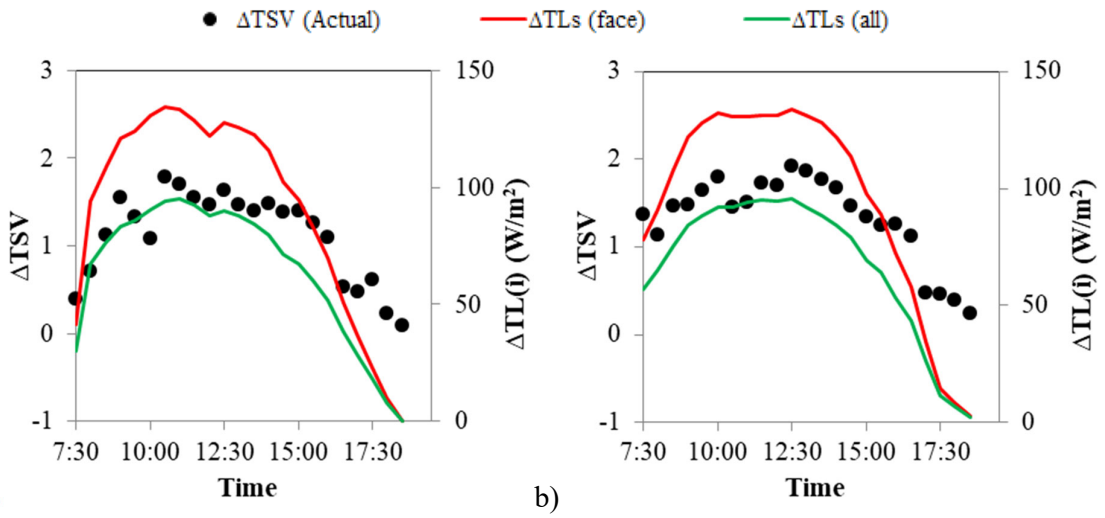

Fig. 4. Input parameters for different thermal comfort models for outdoor case 4 a) the experiment on May 17, b) the experiment on June 1, as specified in Table 2.

Figure 5 compares the actual thermal sensation, Δ*TSV (Actual)*, with the values predicted by Zhou's, PMV, and Lai's models. The Δ*TSV (Actual)* varied from 0 to 1.9. The Δ*TSV* was overestimated by the PMV model under outdoor conditions. This overestimation was due mainly to the large Δ*TLs (all)*. As shown in Figure 4, the Δ*TLs (all)* was greater than 40.0 W/m^2, except for the values obtained after 17:00 in Figure 4(a) and after 15:30 in Figure 4(b). The Δ*TSV (PMV)* calculated by Equation (7) was greater than 1.9 for those data points.

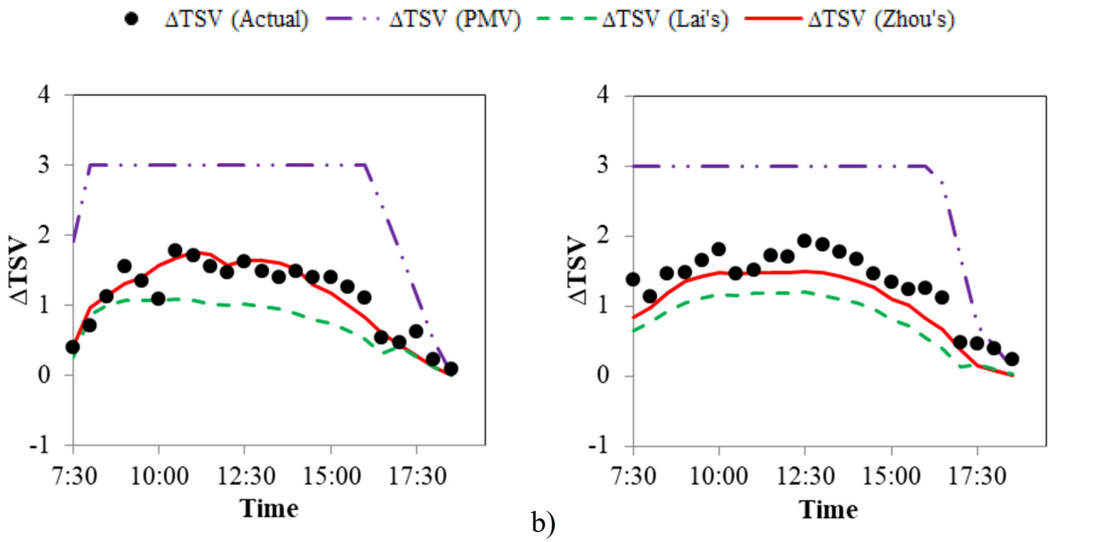

Fig. 5. Comparison of the actual *TSV* changes when shuttling from sun to shade with the predicted changes for outdoor case 4 a) the experiment on May 17, b) the experiment on June 1, as specified in Table 2.

Figure 5 shows that Δ*TSV* was underestimated by Lai's model. According to Equation (8), the Δ*TSV (Lai's)* would change by one unit with a 70.0 W/m^2 change in the Δ*TLs (all)*. Since Δ*TLs (all)* varied from 0 to 95.5 W/m^2, the Δ*TSV (Lai's)* varied from 0.0 to 1.2. Our model yielded the most accurate prediction. According to Equation (5), since Δ*TLs (face)*

varied from 0.0 to 134.2 W/m^2, the ΔTSV *(Zhou's)* varied from 0.0 to 1.8. Sudden changes in thermal load on the face caused by solar radiation can accurately indicate changes in thermal sensation during a transition from sun to umbrella shade with standing posture.

Outdoor case 6: Different solar radiation intensities during exercise

Outdoor case 6[18] investigated the influence of different solar radiation intensities on the thermal sensation of exercising subjects. During the experiments, the subjects first stayed in a laboratory maintained at a comfortable temperature (24–25°C), then went outside, walked for about 20 m to reach an upright cycle ergometer and rested on the ergometer in a seated position for 15 min. After being accustomed to the initial state, subjects performed a 45-min cycling exercise under three sunlight levels: thick cloud (306 ± 52 W/m2, low solar radiation); thin cloud (592 ± 32 W/m^2, medium solar radiation); and clear sky (mean ± SD: 1072 ± 91 W/m2, high solar radiation). Table 7 provides the air and mean radiant temperatures, as well as global solar radiation, air velocity and relative humidity measured under different solar radiation levels[18].

Table 7. Description of outdoor case 6

Phase	T_a (ºC)	T_r (ºC)	G (W/m^2)	V_a (m/s)	SVF	RH (%)	I_{cl} (clo)	$T_{sk,m}$ (ºC)
Low solar radiation	30.8	46.9	306	2.1	0.65	57.0	0.37	32.6-33.9
Medium solar radiation	30.4	48.6	592	1.8	0.65	51.0	0.37	32.8-34.1
High solar radiation	31.0	60.6	1072	2.1	0.65	50.0	0.37	32.9-34.7

Figure 6 compares the actual thermal sensation with the values predicted by Zhou's, PMV, DTS, UCB and Lai's models under low, medium and high solar radiation intensities, respectively. The PMV model over-predicted the outdoor thermal sensation by at least one unit in comparison to the actual *TSV* for a hot outdoor environment. The reason for the higher PMV was the high outdoor thermal load *TL (all)*, as in the previous cases. In addition, Humphreys and Nicol[34] showed that the accuracy of PMV varied according to metabolic rate (*M*), and the PMV model best predicted actual thermal sensation for activity levels below 1.4 met. Above 1.8 met, PMV could overestimate actual thermal sensation by up to one scale unit.

During exercise, the evaporative heat dissipation of sweat had enhanced obviously, the skin temperature would be reduced by sweating. Therefore, the thermal sensations predicted by the DTS and UCB models were significantly smaller than the actual *TSV*. Zhou's and Lai's models accurately predicted the thermal sensations under outdoor exercise conditions. Table 8 presents the *RMSE* for the five models. Zhou's and Lai's models exhibited the best performance with *RMSE* ≤0.5, whereas the other three models did not perform well.

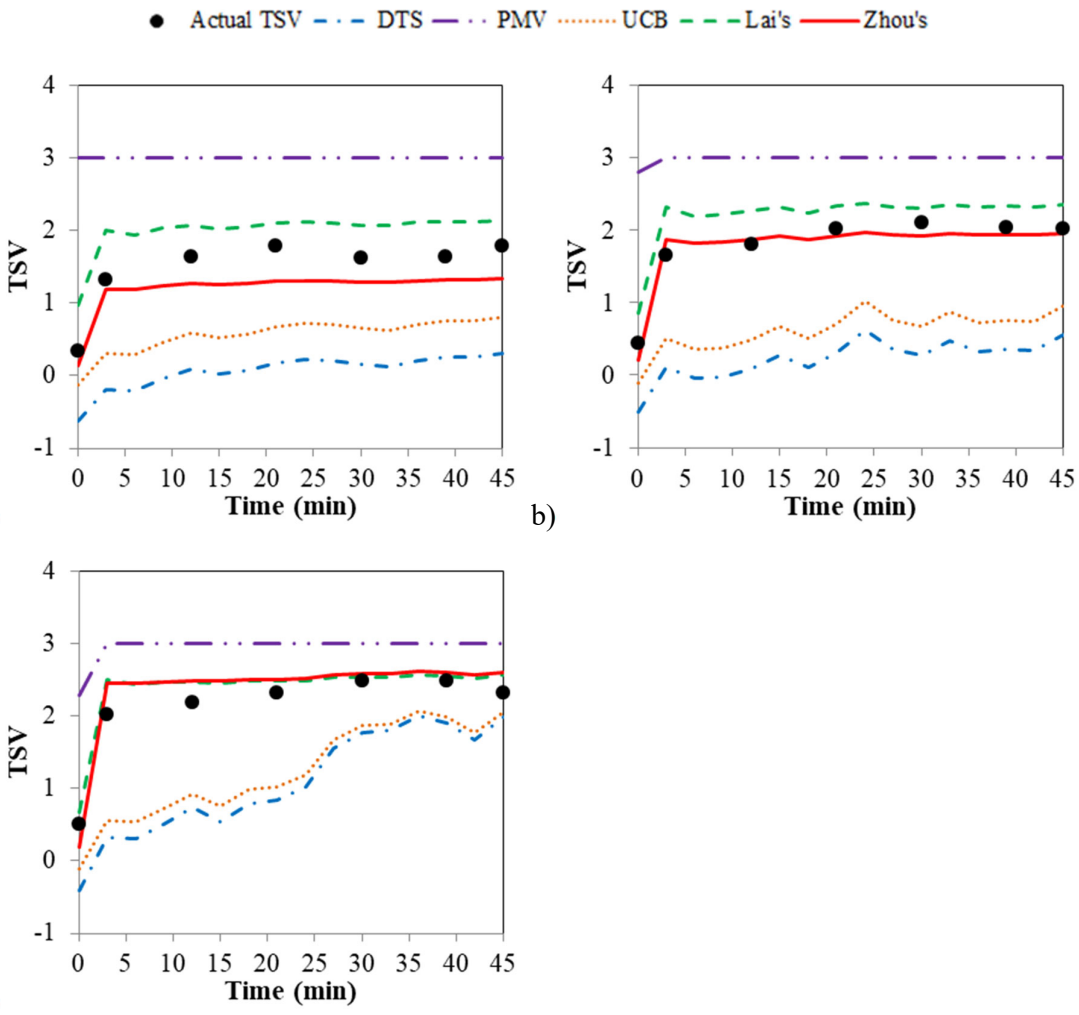

Fig. 6. Comparison of the actual thermal sensation votes with the predicted values for outdoor case 6: a) low solar radiation, b) medium solar radiation, c) high solar radiation, as specified in Table 7.

Table 8. *RMSE* for the five models for outdoor case 6.

	Lai's	PMV	UCB	DTS	Zhou's
Outdoor case 6-1	0.50	1.63	0.94	1.43	0.33
Outdoor case 6-2	0.41	1.33	1.19	1.58	0.15
Outdoor case 6-3	0.23	0.92	0.98	1.15	0.25

Outdoor case 7: Different solar radiation intensities for standing posture

Because of cloud cover, outdoor solar radiation intensity changes frequently. Outdoor case 7[14] investigated the influence of different solar radiation intensities on the thermal sensation of standing subjects. The subjects first stayed in a neutral indoor chamber for 30 min to achieve a stable thermal condition; they then moved to an outdoor space and remained there for 60 min. Table 9 lists the changes in air and mean radiant temperature temperatures over time, as well as global solar radiation, air velocity and relative humidity measured under different levels of solar radiation[14].

Table 9. Description of outdoor case 7

	T_a (ºC)	T_r (ºC)	G (W/m^2)	V_a (m/s)	SVF	RH (%)	I_{cl} (clo)	$T_{sk,m}$ (ºC)
Outdoor case 7-1	34.8	35-48.3	5-400	0.3	0.02-0.65	28.5	0.56	34.0-34.9
Outdoor case 7-2	34.7	35.0-62.0	5-1000	1.3	0.02-0.66	30.5	0.56	34.3-35.5
Outdoor case 7-3	34.2	36.2-47.1	170-400	0.3	0.65	56.0	0.56	34.5-35.4

Figure 7 displays the results calculated with the five thermal sensation models under different solar radiation intensities for the subjects in standing position. Due to the high outdoor air temperature, *TL (all)* was very large. The PMV reached the upper limit of +3 for the four exposure levels. The PMV model was unable to reflect the effects of the sudden change in solar radiation. The DTS and UCB models predicted the trends consistently with the actual trends, but with low accuracy. Since these two models were developed with the use of experimental data obtained under indoor conditions, the performance was not surprising. Lai's and Zhou's models accurately predicted the thermal sensations. Table 10 presents the *RMSE* for the five models. The RMSE values for Lai's, PMV, UCB and DTS models were higher for the outdoor case 7-1 and 7-2 as compared to the outdoor case 7-3. The opposite outcome was observed for Zhou's model. Since case 7 only used one or two subjects, the inter-subject difference may lead to inconsistent prediction accuracy among models. So, we should choose a large subject sample size, and the subjects should encompass a wide variety of ages, weights, or other factors, when selecting verification case.

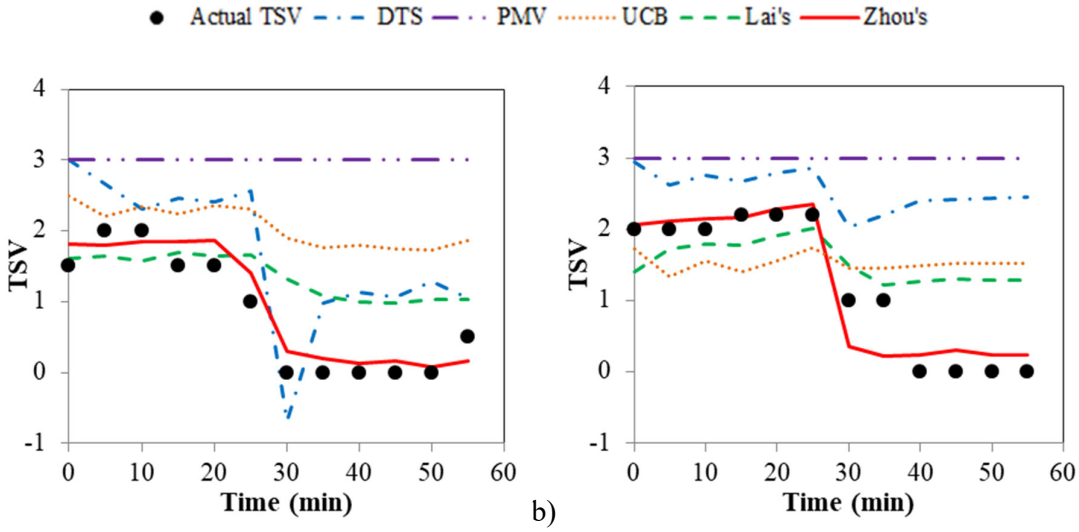

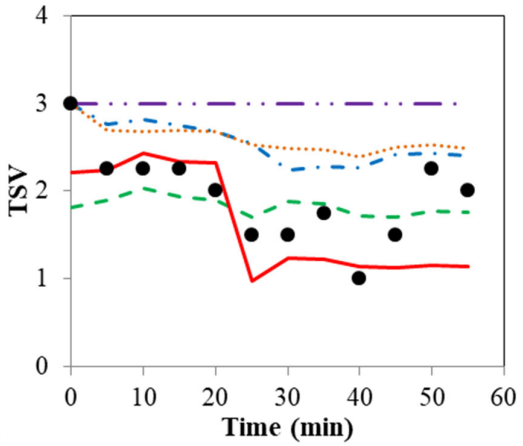

c)

Fig. 7. Comparison of the actual thermal sensation votes with the predicted values for a) outdoor case 7-1, b) outdoor case 7-2, c) outdoor case 7-3, as specified in Table 9.

Table 10. *RMSE* for the five models for outdoor case 7.

	Lai's	PMV	UCB	DTS	Zhou's
Outdoor case 7-1	0.77	2.31	1.35	1.03	0.27
Outdoor case 7-2	0.80	2.02	1.55	1.55	0.34
Outdoor case 7-3	0.48	1.17	0.75	0.70	0.56

Figure 8 is a box chart of *RMSE* for the thermal sensations calculated with the five models for the 11 exposures with sudden changes in solar radiation. Zhou's model was the most accurate with a mean *RMSE* of 0.40 for the 11 cases. Lai's model was also very good with a mean *RMSE* of 0.68. Lai's model did not perform as well as Zhou's because the former was based on data from subjects facing away from the sun. The high outdoor temperature and solar radiation intensity deviated greatly from the neutral state, causing the PMV model to overestimate the thermal sensation. The DTS and UCB models failed to predict the temporal *TSV* changes due to sudden changes in solar radiation because the two models use skin and core temperatures as inputs, and these parameters changed only slightly with the solar radiation.

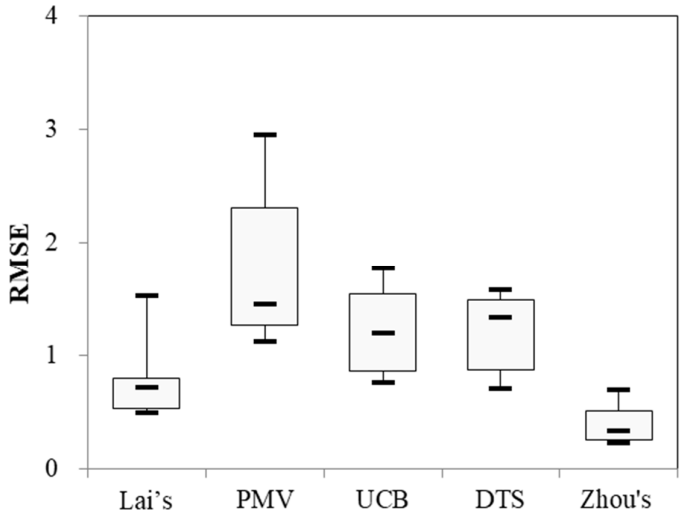

Fig. 8. Box chart of *RMSE* for thermal sensation predictions from the models for 11 outdoor exposures. (The horizontal line represents the median value, the lower and upper bounds of the boxes represent the 25th and 75th percentiles, respectively, and the lower and upper bars indicate the minimum and maximum, respectively.)

3.2 Validation of indoor cases

Due to space limitations, this section presents the evaluation results for a typical indoor case with air temperature ramps and an indoor case with a step change in air temperature. The complete evaluation results are then summarized.

Indoor case 2: Air temperature ramps

The evaluation of thermal sensation in environments with air temperature ramps is important because this situation is frequently encountered in indoor spaces, e.g., in a naturally ventilated building where the indoor air temperature changes gradually with the outdoor temperature, or in a room where the air temperature gradually increases or decreases when the target set temperature changes[35]. In the selected validation cases in Table 3, the rate of temperature change ranged from 4 K/h to 12 K/h.

Indoor case 2[23] studied human thermal sensation in response to two dynamic temperature changes. One was a gradual increase in temperature (+ 4 K/h, ranging from 24 to 32 °C). The actual *TSV* and the results predicted by the five models for this exposure scenario are displayed in Figure 9(a). The other change was a gradual decrease in temperature (− 4 K/h, ranging from 24 to 16 °C), and the results are shown in Figure 9(b).

For the transient period, it can be seen that the PMV model correctly reproduced the trend of change, whereas the other models predicted a faster or slower increase/decrease in thermal sensation than the actual trend. As shown in Table 11, the *RMSE* values from all models were lower than 1.0 unit. The prediction accuracy of the UCB model was poor in the thermal environment with an air temperature of 24 ºC. This was mainly because the actual *TSV* indicated a neutral state, with a voting value of 0.0–0.5, but the lower skin temperature caused the UCB model to predict a value of-1.0.

During the gradual two-hour temperature change, the trend of the skin temperature change was consistent with that of the air temperature change. Therefore, the errors between the values predicted by the DTS and Lai's models and the experimental value were small, and the *RMSE* values were less than0.60. Since Zhou's model was obtained by regression using experimental data obtained under different thermal environments in vehicles, with an

applicable temperature range of 0–50 ºC, the sensitivity was poor when the model was used for indoor cases.

Among the five models, the PMV model had the highest accuracy, mainly because an environment can be regarded approximately as steady-state when the temperature change is small. For temperature ramps, the ISO 7730 standard (ISO 2005)[19] recommends the use of a steady-state evaluation method (such as the PMV model) if the temperature change is less than 2 K/h. Knudsen et al.[36] addressed the possibility of using the PMV model to predict thermal sensation during temperature ramps up to ±5 K/h.

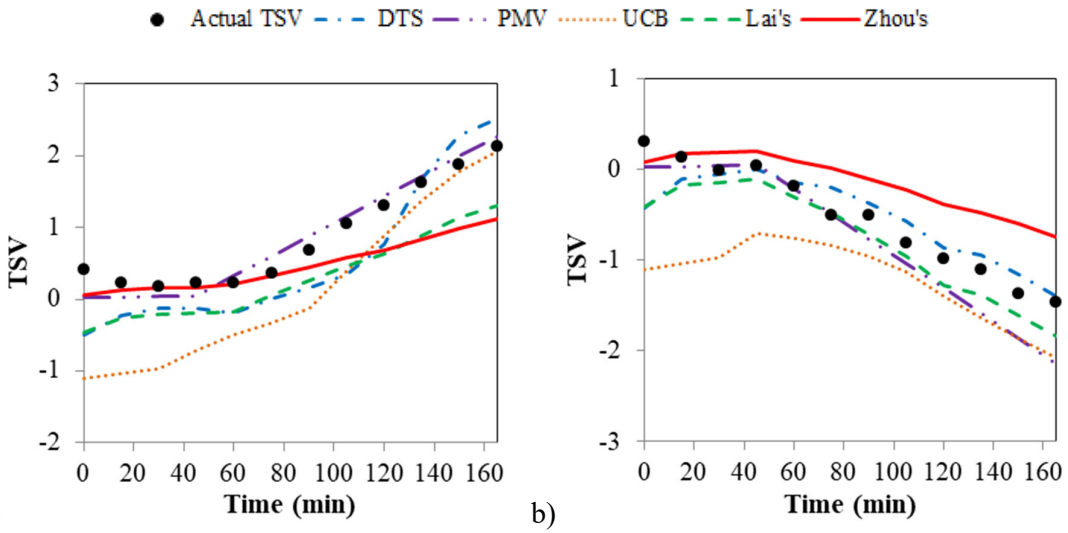

Fig. 9. Comparison of the actual thermal sensation votes with the predicted values for an air temperature ramp-change: a) 24-32 ºC (+4º C/h), b) 24-16 ºC (-4º C/h) (indoor case 2 in Table 3).

Table 11. *RMSE* for the five models for indoor case 2.

	Lai's	PMV	UCB	DTS	Zhou's
Indoor case 2-1	0.60	0.18	0.84	0.49	0.52
Indoor case 2-2	0.30	0.32	0.74	0.26	0.48

The validation results for another case with air temperature ramps (indoor case 1) were similar. The validation process will not be repeated here.

Indoor case 4: Step change in air temperature

We selected indoor case 4[26] as a typical case because it included multiple types of thermal environments, and each exposure scenario contained two temperature step changes, upward and downward.

Four air temperature step-change cases are presented here. Two of them represent an environmental change from neutral to warm/slightly warm and back to neutral, while the other two represent an environmental change from neutral to cool/slightly cool and back to neutral. These situations are often encountered in daily life.

Figure 10 compares the experimental *TSV* with that calculated by the five models, for indoor cases 4-1 to 4-4. Each model was able to predict the change trend of *TSV*, but their performance varied. Table 12 shows the root mean square error (*RMSE*) between the predicted value from each of the thermal sensation models and the experimental value. The PMV model had the highest accuracy among the five models, with *RMSE* values lower than 0.7 for the four cases. There was a delay in skin temperature in response to drastic external

change. In terms of the time of response, thermal load offers advantages to predict human thermal sensation, when people undergo temperature step change. The results of Liu et al.[27] in step change experiments (warm-neutral-warm) and Du et al.[37] in step change experiments (cool-neutral-cool) both showed a linear correlation between *TSV* and *TL* in such transient environment.

Table 12. *RMSE* for the five models for indoor case 4.

	Lai's	PMV	UCB	DTS	Zhou's
Indoor case 4-1	0.75	0.67	0.83	1.13	0.77
Indoor case 4-2	0.52	0.48	0.69	1.02	0.51
Indoor case 4-3	0.71	0.29	0.60	0.78	0.73
Indoor case 4-4	1.07	0.63	0.99	1.10	0.98

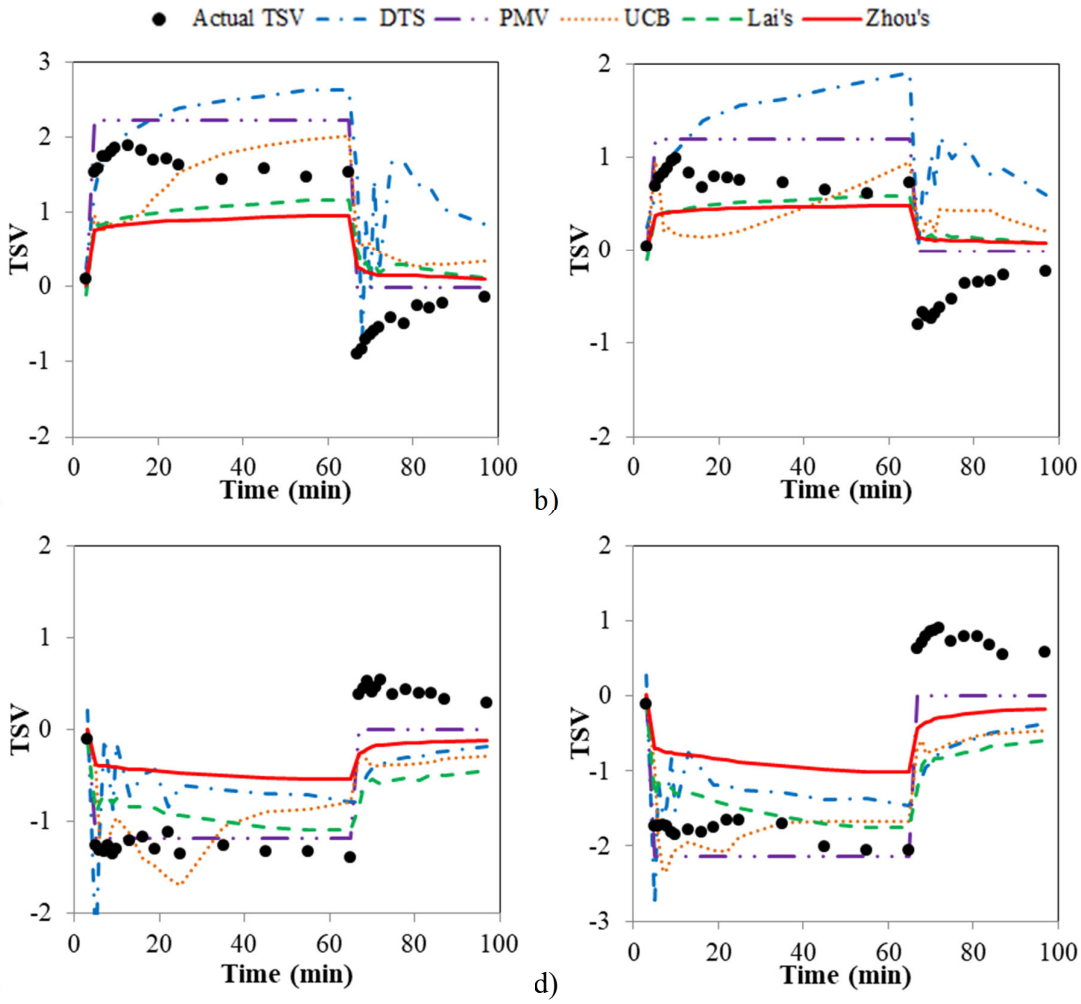

Fig. 10. Comparison of the actual thermal sensation votes with the predicted values for an air temperature step-change: a) 26-32-26 ºC, b) 26-29-26 ºC, c) 26-23-26 ºC, d) 26-20-26 ºC (indoor case 4 in Table 3).

For all five thermal comfort models, the RMSE values for case 4-2 (with air temperature step-changes of 26–29–26 ºC) and for case 4-3 (26–23–26 ºC) were smaller than those for

case 4-1 (26–32–26 ºC) and case 4-4 (26–20–26 ºC). That is, the accuracy of all five thermal comfort model predictions for the 3 K temperature steps was higher than their accuracy for the 6 K steps. Larger deviation from neutral can be observed for case 4-1 and case 4-4 than case 4-2 and 4-3. It can be seen that the above five models had high prediction accuracy around neutral state. While beyond the neutral state, the prediction accuracy for thermal comfort models still suffers[38].

For each exposure scenario, the accuracy of the five models in predicting thermal sensation after the transition from a neutral to a non-neutral environment was significantly higher than that in predicting the thermal sensation after the transition from a non-neutral to a neutral environment. This is mainly because the human thermal sensation response is more sensitive and effective in the non-neutral to neutral step than in the neutral to non-neutral step, which would be caused by the large effect of thermal experience on thermal sensation. However, none of the five models could accurately predict this change. Further research on dynamic thermal sensation modeling should consider the accurate modeling of the effect thermal experience.

The validation results for another case with an air temperature step change yielded similar results. In the PMV, Lai's and Zhou's models, thermal load or the thermal load of the face was used as an important indicator of thermal sensation, as it could reflect the sudden change in thermal sensation when a sudden change in air temperature occurs. Meanwhile, the UCB and DTS models mainly used skin temperature and skin temperature change rate to predict thermal sensation, and exhibited poor response to sudden change. The prediction accuracy of the UCB and DTS models was lower than that of the other three models. The validation process will not be repeated here.

Figure 11 is a box chart of root-mean-square error (*RMSE*) for thermal sensation predictions from the models for 20 exposure scenarios. It can be seen that for the 20 indoor cases chosen for validation, the PMV model had the highest accuracy among the five comparison models, with a mean *RMSE* value of 0.57 for the 20 cases. Zhou's and Lai's models yielded highly accurate predictions, with mean *RMSE* values of 0.65 and 0.82, respectively, for the 20 cases. For the UCB model, the mean *RMSE* value was 1.02. For the DTS model, it was 1.10.

In order to further investigate the differences in prediction accuracy among different models, we re-analyzed the 20 indoor validation cases. We found that, with the exception of cases 6-1, 6-2, 8-1 and 8-2, the environmental parameters of the remaining 16 cases were primarily concentrated as follows: air temperature equal to mean radiant temperature from 20 to 32 °C, relative humidity of 50%, air velocity of 0.1 m/s, and clothing thermal insulation of 0.50 clo. Next, the physiological parameters during exposure to these thermal environments, which were required for the computation of the DTS, UCB, Lai's, and Zhou's predictions, were obtained from thermo-physiological simulations with the thermoregulation model by Fiala[39]. This model was chosen because it has been extensively validated for a wide range of conditions[40].

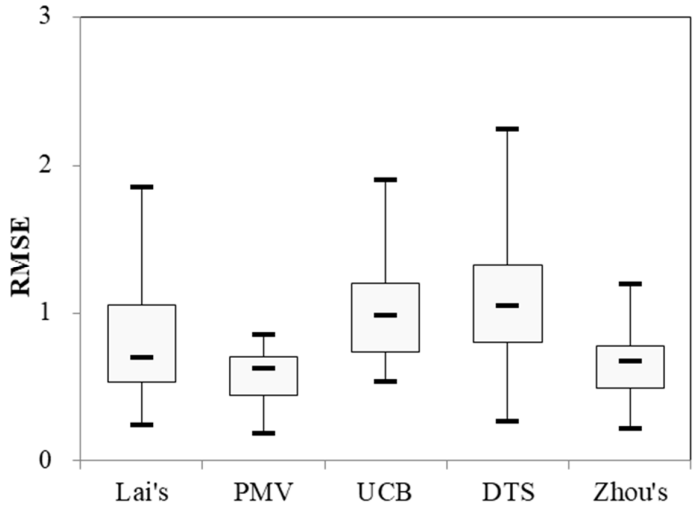

Fig. 11. Box chart of root-mean-square error (*RMSE*) for thermal sensation predictions from the models for 20 indoor exposure scenarios presented in thermal sensation units. (The horizontal line represents the median value, the lower and upper bounds of the boxes represent the 25th and 75th percentiles, respectively, and the lower and upper bars indicate the minimum and maximum, respectively).

Figure 12 shows five thermal sensation predictions after 60 min of exposure with wind speed of 0.1 m/s, relative humidity of 50%, clothing thermal insulation of 0.50 clo and metabolic rate of 1.0 met. The thermal sensation value predicted by the PMV model is 0 when T_a = 24.0 ºC. The predicted value would change one unit with an air temperature change of about 3.5 ºC. The slope of the PMV model is similar to the slopes of the UCB, DTS and Lai's models. However, the thermal sensation values predicted by the UCB, DTS and Lai's models were 0 with T_a = 26.0, 28.0, 22.0 ºC. Meanwhile, the thermal sensation value predicted by Zhou's model is 0 when T_a = 24.0 ºC. The predicted value would change one unit with an air temperature change of about 7.0 ºC. Zhou's model has the lowest slope, which means that it is the least sensitive to temperature.

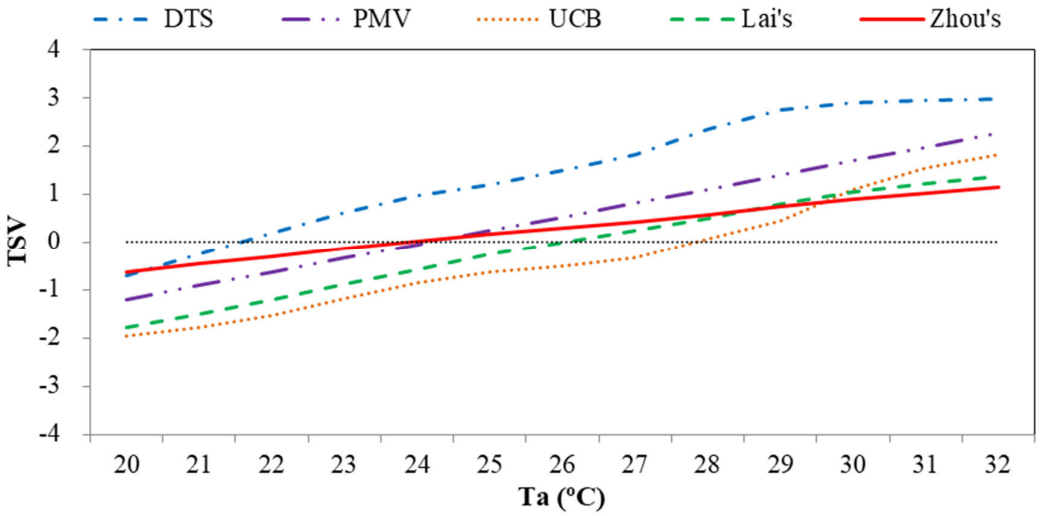

Fig. 12. Thermal sensation predictions after 60 min of exposure with wind speed of 0.1 m/s, relative humidity of 50%, clothing thermal insulation of 0.5 clo and metabolic rate of 1.0 met.

For most of the indoor cases selected for validation, the thermal environment fell within the applicable scope of the PMV model (19–28º C from Table 1). This explains why the PMV model exhibits the highest prediction accuracy. When the PMV model is used as a reference, it can be seen in Figure 12 that Lai's and Zhou's models deviate less from the PMV model than do the UCB and DTS models. The *RMSE* between the predicted value of the DTS model and the PMV model is 0.95, while it is 0.72 for the UCB model, 0.38 for Lai's model, and 0.34 for Zhou's model.

Therefore, when the thermal environment is in a neutral state or deviates moderately from neutral (T_a = 20–32 ºC), whether there is a temperature gradient change or a temperature step change, the PMV model exhibits the highest accuracy in predicting thermal sensation.

4. Discussion

4.1 *TLs (face)* and *TLs (all)*

This paper has verified the effects of sudden changes in solar radiation on the thermal perception, as described in Section 3.1, which result from the transition between sunlight and shade. We will now discuss another outdoor situation, that is, the effects of the azimuth angle between the human body and the sun on thermal sensation. In the outdoor-case analyses in Section 3.1, it was found that the *TLs (all)* or *TLs (face)* plays a major role in thermal sensation.

Figure 13 shows the *TLs (face)* and *TLs (all)* results from January 22. The red and black solid lines refer to *TLs (face)* and *TLs (all)*, respectively, when subjects are standing and facing the sun. The red and black dashed lines refer to *TLs (face)* and *TLs (all)*, respectively, when subjects' backs are toward the sun. The *TLs (face)* was always greater than *TLs (all)*, and the difference between *TLs (face)* and *TLs (all)* reached a maximum at 93.8 W/m^2, when subjects were facing the sun (azimuth = 0º). Meanwhile, *TLs (face)* was always lower than *TLs (all)*, and the difference between *TLs (face)* and *TLs (all)* reached a minimum at -59.5 W/m^2, when subjects had their backs toward the sun (azimuth = 180º). Therefore, *TLs (face)* is very sensitive to the azimuth angle.

In Figure 13, we also see the difference between the solar radiation thermal load of the face when subjects were facing the sun (azimuth = 0º) and had their backs toward the sun (azimuth = 180º). The Δ*TLs (face)* varied from 0 to 166.4 W/m^2, while the Δ*TLs (all)* varied from -1.3 to 13.0 W/m^2. This also explains why the *TSV* difference reached 1–2 units between facing the sun and back toward the sun. The other models (such as PMV and Lai's) did not reflect this difference.

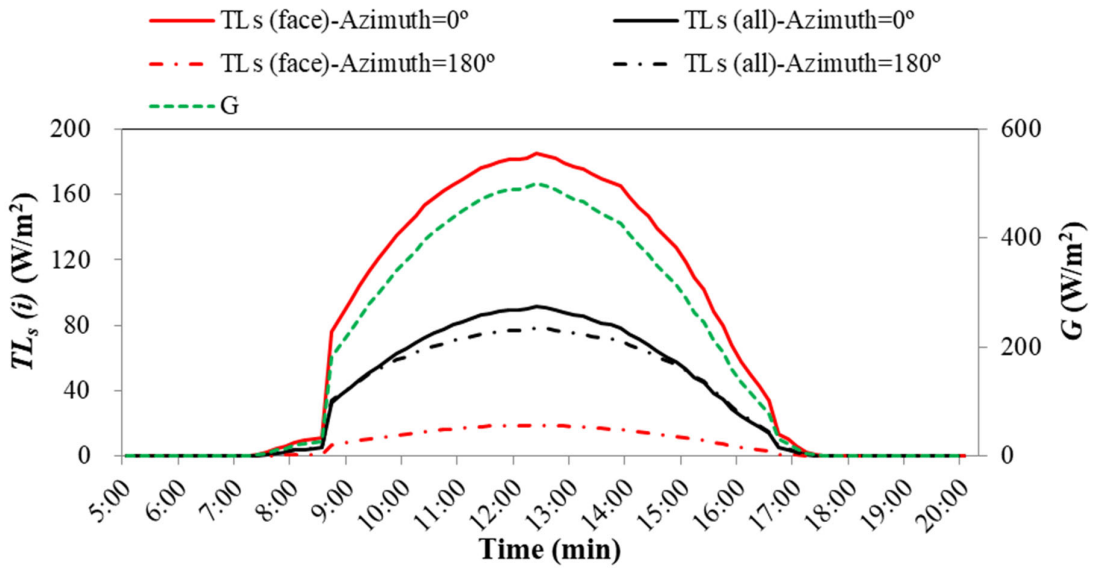

Fig. 13. The *TLs (face)* and *TLs (all)* results on January 22.

Table 13 presents the results for 12 typical days throughout the year in Tianjin, China. It can be seen that the maximum difference between the solar radiation thermal load of the face when subjects were facing the sun (azimuth = 0°) and had their backs toward the sun (azimuth = 180°), Δ*TLs (face)*, varied from 135.5 to 167.3 W/m^2, while the Δ*TLs (all)* varied from 10.0 to 30.0 W/m^2 throughout the year.

Assuming that the person is in a standing posture outdoors, the *TSV* difference between facing the sun and back toward the sun throughout the year can be calculated by Eqs. (5), (7) and (8). The *TSV* difference between facing the sun and back toward the sun, calculated by Zhou's model, can reach 1–2 units throughout the year. According to Lai's model, however, the difference is less than 0.5 units. Since the value of *TLs (all)* was very large, the PMV model still reached the upper limit of +3, and it did not reflect the *TSV* difference between facing the sun and back toward the sun.

Table 13. The *TLs (face)* and *TLs (all)* results throughout the year.

Date	*G* (W/m^2)	Azimuth = 0°		Azimuth = 180°		Maximum	
		TLs (face) (W/m^2)	*TLs (all)* (W/m^2)	*TLs (face)* (W/m^2)	*TLs (all)* (W/m^2)	Δ*TLs (face)* (W/m^2)	Δ*TLs (all)* (W/m^2)
0122	0-500	185.3	91.5	19.0	78.5	166.3	13.0
0222	0-480	153.2	84.7	18.2	66.6	135.5	18.2
0322	0-631	170.0	97.8	24.0	72.5	148.5	26.1
0422	0-914	192.9	128.8	34.7	99.5	167.3	32.2
0522	0-914	183.2	111.7	35.3	95.4	158.6	28.0
0622	0-868	182.9	103.1	32.9	88.2	159.9	26.3
0722	0-824	175.2	99.9	31.3	84.6	152.8	24.9
0822	0-820	177.4	105.8	31.1	82.1	152.9	26.6
0922	0-700	186.8	108.5	26.5	79.7	163.1	28.8
1022	0-524	167.7	86.8	19.9	68.4	147.9	18.5
1122	0-453	162.4	82.4	17.2	69.1	145.2	13.3
1222	0-456	169.2	83.5	17.3	71.7	151.9	11.8

4.2 Limitations and future challenges

The core temperature of the human body is an important physiological parameter that influences thermal sensation. In practice, body core temperature is commonly monitored through rectal, esophageal, or tympanic measurements. Human beings are homeotherms, therefore, in different environment, even in extreme cold or hot, people can maintain core temperature in a narrow scope through thermoregulation. The core temperature is kept at about 36.5°C [41]. Lind [42] showed that core temperature was independent of environmental temperature under cold-to-moderate conditions. Therefore, we did not consider core temperature as a key consideration when we performed model verification.

The selected validation cases represented transient environments. It was found that the accuracy of Zhou's model was very high in an outdoor or vehicular environment where there was a sudden change in solar radiation.

In light of the selected cases, the following problems arise:

1. The outdoor validation cases, where there was a sudden change in solar radiation, were carried out mainly in a warm or hot environment. There are very few studies in the literature that address winter conditions, that is, cases in which a cool or cold environment is considered.
2. The indoor validation cases, where there was a temperature gradient change or a temperature step change, were carried out mainly in a neutral state or with moderate deviation from the neutral environment. There are very few cases of severe deviation from the neutral environment in the literature.

It is still unknown whether the newly developed Zhou's model can be used in the above-mentioned thermal environments for which the existing literature is scarce.

5. Conclusions

Our previous work developed a model (Zhou's) to predict thermal sensation in a transient and non-uniform vehicular thermal environment. The present study was designed to evaluate the application of this model to other non-uniform and transient environments.

The accuracy of the newly developed thermal sensation model (Zhou's) and four other selected thermal comfort models has been evaluated through a validation study for outdoor spaces (11exposure scenarios), and indoor spaces with air temperature ramps (three scenarios), and step changes (17 scenarios).

All the investigated models, with the exception of Zhou's and Lai's, exhibit low accuracy (*RMSE* larger than 1 unit) for the twelve outdoor cases. Zhou's model yields the most accurate prediction for the outdoor cases, with a mean *RMSE* value for twelve cases of 0.40.

The trend of thermal changes can be predicted by Zhou's model, but the accuracy is lower than that of the PMV model for a neutral state or with moderate deviation from neutral (T_a = 20–32 ºC), whether there is a temperature gradient change or a temperature step change.

The *TSV* when subjects are facing the sun can differ by as much as 1–2 units from the *TSV* when subjects have their backs toward the sun, because of the difference in solar radiation thermal load on the face, ΔTL_s *(face)*. The other models (such as PMV and Lai's) cannot reflect this difference.

Acknowledgement

This study was supported by the National Key R&D Program of the Ministry of Science and Technology, China, on “Green Buildings and Building Industrialization” through Grant 2018YFC0705300.

References

[1] Zhang H. 2004. Human thermal sensation and comfort in transient and non-uniform thermal environments. Ph.D. Thesis. University of California at Berkeley, CA, USA.

[2] Zhou X, Lai D, Chen Q. Experimental investigation of thermal comfort in a passenger car under driving conditions. Building and Environment 149 (2019) 109–119.

[3] Zhou X, Liu S, Liu X, et al. Evaluation of four models for predicting thermal sensation in Chinese residential kitchen. CLIMA 2019, May 26-29, 2019, Bucharest, Romania.

[4] Fiala D (1998) Dynamic simulation of human heat transfer and thermal comfort. PhD thesis, De Montfort University, UK.

[5] Fiala D, Lomas K, Stohrer M. First principles modeling of thermal sensation responses in steady-state and transient conditions. ASHRAE Transactions 109 (2003) 179–186.

[6] Zhang H, Arens E, Huizenga C, Han T. Thermal sensation and comfort models for non-uniform and transient environments: Part I: Local sensation of individual body parts. Building and Environment 45 (2010) 380–388.

[7] Zhang H, Arens E, Huizenga C, Han T. Thermal sensation and comfort models for non-uniform and transient environments, Part III: Whole-body sensation and comfort. Building and Environment 45 (2010) 399–410.

[8] Lai D, Chen Q. A two-dimensional model for calculating heat transfer in the human body in a transient and non-uniform thermal environment. Energy and Buildings 118 (2016) 114–122.

[9] Lai D, Zhou X, Chen Q. Modelling dynamic thermal sensation of human subjects in outdoor environments. Energy and Buildings 149 (2017) 16–25.

[10] Zhou X, Lai D, Chen Q.Thermal sensation model for driver in a passenger car with changing solar radiation. Building and Environment 183 (2020) 107219.

[11] Fanger PO. 1970. Thermal Comfort. Copenhagen: Danish Technical Press.

[12] Koelblen B, Psikuta A, Bogdan A, et al. Thermal sensation models: A systematic comparison. Indoor Air 27 (2017) 680–689.

[13] Watanabe S, Nagano K, Ishii J, Horikoshi T. Evaluation of outdoor thermal comfort in sunlight, building shade, and pergola shade during summer in a humid subtropical region. Building and Environment 82 (2014) 556–565.

[14] Lai D, Zhou X, Chen Q. Measurements and predictions of the skin temperature of human subjects on outdoor environment. Energy and Buildings 151 (2017) 476–486.

[15] Shimazaki Y, Yoshida A, Suzuki R, et al. Application of human thermal load into unsteady condition for improvement of outdoor thermal comfort. Building and Environment 46 (2011) 1716–1724.

[16] Givonia B, Noguchi M, Saaronic H, et al. Outdoor comfort research issues. Energy and Buildings 35 (2003) 77–86.

[17] Yoshida A, Hayashi D, Shimazaki Y, Kinoshita S. Evaluation of thermal sensation in various outdoor radiation environments. Architectural Science Review 62 (3) (2019) 261–270.

[18] Otani H, Kaya M, Tamaki A, et al. Exposure to high solar radiation reduces self-regulated exercise intensity in the heat outdoors. Physiology & Behavior 199 (2019) 191–199.

[19] ISO7730 2005, International standard: Ergonomics of the Thermal Environment-Analytical Determination of Thermal Comfort by Using Calculations of the PMV and PPD Indices and Local Thermal Comfort Criteria. Geneva: International Organization for Standardization.

[20] Rupp RF, Vásquez NG, Lamberts R. A review of human thermal comfort in the built environment. Energy and Buildings 105 (2015) 178–205.

[21] Craenendonck SV, Lauriks L, Vuye C, et al. A review of human thermal comfort experiments in controlled and semi-controlled environments. Renewable and Sustainable Energy Reviews 82 (2018) 3365–3378.
[22] Yasuoka A, Kubo H, KazuyoTsuzuki K, Isoda N. Interindividual differences in thermal comfort and the responses to skin cooling in young women. Journal of Thermal Biology 37 (2012) 65–71.
[23] Jacquot CM, Schellen L, Kingma BR, et al. Influence of thermophysiology on thermal behavior: The essentials of categorization. Physiology & Behavior 128 (2014) 180–187.
[24] Xiong J, Zhou X, Lian Z, et al. Thermal perception and skin temperature in different transient thermal environments in summer. Energy and Buildings 128 (2016) 155–163.
[25] Xiong J, Lian Z, Zhou X, et al. Effects of temperature steps on human health and thermal comfort. Building and Environment 94 (2015) 144–154.
[26] Zhang Z, Zhang Y, Ding E. Acceptable temperature steps for transitional spaces in the hot-humid area of China. Building and Environment 121 (2017) 190–199.
[27] Liu H, Liao J, Yang D, et al. The response of human thermal perception and skin temperature to step-change transient thermal environments. Building and Environment 73 (2014) 232–238.
[28] Gagge AP, Stolwijk JAJ, Hardy JD.Comfort and Thermal Sensations and Associated Physiological Responses at Various Ambient Temperatures. Environmental Research 1 (1) (1967) 1–20.
[29] Chen C, Hwang R, Chang S, Lu Y. Effects of temperature steps on human skin physiology and thermal sensation response. Building and Environment 46 (2011) 2387–2397.
[30] Velt KB, Daanen HAM. Thermal sensation and thermal comfort in changing environments. Journal of Building Engineering 10 (2017) 42–46.
[31] Nikolopoulou M, Baker N, Steemers K. Thermal comfort in outdoor urbanspaces: Understanding the human parameter, Solar Energy 70 (3) (2001)227–235.
[32] Thorsson S, Lindqvist M, Lindqvist S. Thermal bioclimatic conditions andpatterns of behavior in an urban park in Goteborg, Sweden, Int. J. Biometeorol 48 (3) (2004) 149–156.
[33] Lai D, Guo D, Hou Y, et al. Studies of outdoor thermal comfort in northern China, Building and Environment 77 (2014) 110–118.
[34] Humphreys MA, Nicol JF. The validity of ISO-PMV for predicting comfort votes in everyday thermal environments, Energy and Buildings 34 (6) (2002) 667–684.
[35] Koelblen B, Psikuta A, Bogdan A, et al. Thermal sensation models: Validation and sensitivity towards thermo-physiological parameters. Building and Environment 130 (2018) 200–211.
[36] Knudsen HN, Fanger PO. 1989. Thermal comfort in passive solar buildings. CEC Research Project: EN3S-0035-DK(B), Laboratory of Heating and Air Conditioning, Technical University of Denmark, Copenhagen, Denmark.
[37] Du X, Li B, Liu H, et al. The Response of Human Thermal Sensation and Its Prediction to Temperature Step-Change (Cool-Neutral-Cool). PLoS ONE 9 (8): e104320.
[38] Wenzel HG, Mehnert C, Schwarzenau P. Evaluation of tolerance limits for humans under heat stress and the problems involved. Scand J Work Environ Health 15 (1) (1989) 7–14.
[39] Psikuta A, Fiala D, Laschewski G, et al. Validation of the Fiala mul-node thermophysiological model for UTCI applica on. Int J Biometeorol 56 (2012) 443–460.
[40] Katavoutas G, Flocas HA, Matzarakis A, Dynamic modeling of human thermal comfort after the transition from an indoor to an outdoor hot environment, Int. J. Biometeorol 59 (2) (2015) 205–216.

[41] Choi JH, Loftness V. Investigation of human body skin temperatures as a bio-signal to indicate overall thermal sensations. Building and Environment 58 (2012) 258–269.
[42] Lind AR. A physiological criterion for setting thermal environmental limits for everyday work. Journal of Applied Physiology 18 (1963) 51–56.